Quasielastic γ-ray scattering from pentadecane

G. Schupp, B. Hammouda,* and C. M. Hsueh†
Department of Physics and Research Reactor, University of Missouri–Columbia, Columbia, Missouri 65211
(Received 11 October 1988; revised manuscript received 13 November 1989)

A recently developed Mössbauer instrument has been used to study the liquid dynamics of pentadecane at various temperatures and scattering angles. Widths of the quasielastic signal extracted from the data ranged between 16 GHz (at 12 °C) and 48 GHz (at 74 °C) at a scattering vector of 1.15 Å^{-1}. Similar measurements at five different scattering angles (at 12 °C) were also taken to investigate the Q dependence between 0.82 and 1.56 Å^{-1}. The results obtained are in good agreement with classical theory for coherent scattering from liquids.

INTRODUCTION

Quasielastic scattering of various forms of radiation has been a valuable diagnostic probe to investigate liquids and solutions. Quasielastic light scattering (QELS) has been a useful tool to study normal modes in various viscous systems[1] and is characterized by small scattering vectors. It has been used in frequency domain (Rayleigh scattering) to investigate dynamics with frequency scales in the gigahertz range or to probe time scales in the millisecond range. Quasielastic neutron scattering (QENS) has also been possible with high-energy resolution spectrometers,[2] (meV to μeV) such as backscattering, time of flight, etc., that measure $S(Q,\omega)$, or to the neutron spin-echo technique (sub-μeV) that measures the intermediate scattering function, $I(Q,t)$, directly. Isotope labeling can sometimes provide a means of separating coherent and incoherent contributions. The present experiments used a quasielastic γ-ray scattering (QEGS) instrument[3] recently constructed at the Missouri University Research Reactor (MURR), which utilizes high-intensity Mössbauer sources to give energy resolutions in the GHz (or μeV) range. This instrument has recently been used in investigations where the high-energy resolution was required.[4,5]

Scattering experiments with momentum and energy transfers are described by the dynamic structure factor $S(Q,\omega)$, where Q is the magnitude of the scattering vector $|\mathbf{k}_f-\mathbf{k}_i|$, and $\hbar\omega$ is the energy transfer E_f-E_i. $S(Q,\omega)$ is the time Fourier transform of the intermediate scattering function $I(Q,t)$ given by

$$I(\mathbf{Q},t)=(1/N)\langle\rho^*(Q,0)\rho(Q,t)\rangle ,$$

where N represents the number of scatterers in the sample and $\rho(Q,t)=\sum_i \exp[i\mathbf{Q}\cdot\mathbf{r}_i(t)]$ is the stochastic scattering density.[6] Assuming an exponentially decaying form for $I(Q,t)$ as $S(Q)\exp[-\Gamma(Q)|t|]$ leads to a Lorentzian shape for $S(Q,\omega)$ given by

$$S(Q,\omega)=S(Q)(1/\pi)\Gamma(Q)/[\omega^2+\Gamma(Q)^2] .$$

Sum rules relate the frequency moments of $S(Q,\omega)$ to physical characteristics of the system. For a simple coherent scatterer, the zeroth and second moments are given, respectively, by

$$\langle\omega^0\rangle=\int d\omega\, S(Q,\omega)=S(Q),$$
$$\langle\omega^2\rangle=\int d\omega\,\omega^2 S(Q,\omega)=Q^2k_BT/M ,$$

where M is an appropriately weighted scatterer mass and $S(Q)$ is the static structure factor. No quantum-mechanical effects have been included since $\hbar\omega/k_BT\ll 1$ for quasielastic scattering in general. It should be noted that the commonly used exponential form for $I(Q,t)$ presented above cannot describe the very fast ($\omega\to\infty$) modes. While these modes are not sampled experimentally, the simple exponential model $\exp[-\Gamma(Q)|t|]$, does not give a well-defined first moment $\langle\omega^1\rangle$ as $t\to 0$. The quasielastic width [half-width at half-maximum (HWHM)] $\Gamma(Q)$ can be related to the frequency moments by

$$\Gamma(Q)=(\langle\omega^2\rangle/\langle\omega^0\rangle)^{1/2}=[Q^2k_BT/MS(Q)]^{1/2} . \quad (1)$$

Liquids are dominated by thermal Brownian motion which leads to quasielastic-inelastic scattering processes.[6,7] Mössbauer studies of diffusion in liquids were first conducted for ^{57}Fe ions dispersed in glycerol by Bunbury *et al.*[8] and Craig and Suttin.[9] Until the development of the QEGS instrument, however, studies of this type were limited to liquids which included the Mössbauer nuclide. Pentadecane was chosen to demonstrate this new technique in the present experiments because its melting point at 10 °C afforded an easily accessible temperature range and its quasielastic broadening was appropriate for investigation with QEGS. At room temperature, with a scattering angle corresponding to the first maximum of the structure factor, the quasielastic width was found to be 21 GHz. When the temperature was decreased below freezing, the width collapsed to the instrumental resolution of 1.8 GHz; at 74 °C the width was 48 GHz.

EXPERIMENTAL PROCEDURES

The QEGS instrument[3] is a γ-ray diffractometer which uses intense Mössbauer sources cooled to 77 K. A schematic drawing of QEGS is shown in Fig. 1. Most of

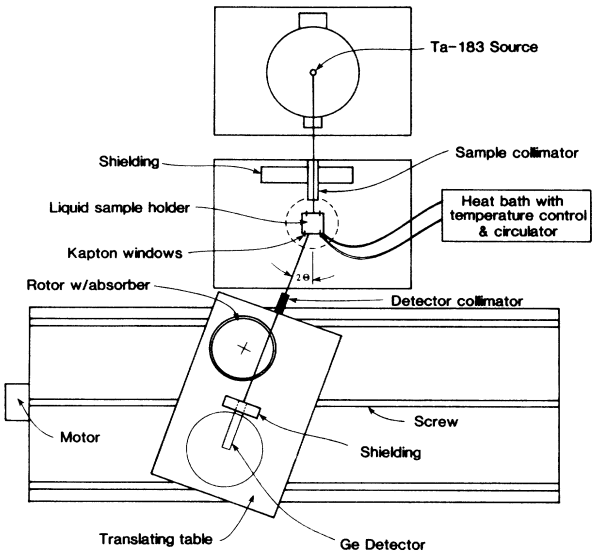

FIG. 1. Schematic drawing of the QEGS instrument. The drawing is approximately to scale with a source-sample distance of 71 cm.

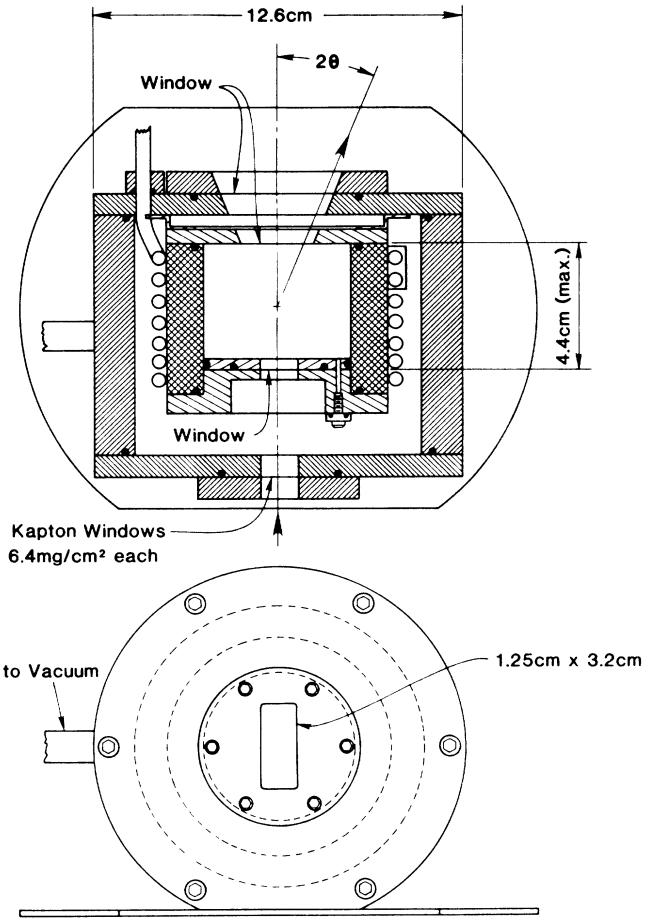

FIG. 2. Liquid sample cell. The inner cell is made of copper with stainless-steel ends while the outer vacuum enclosure is of aluminum.

the work to date has used 70 Ci, 5.1 day ^{183}Ta sources produced by successive neutron capture in the Missouri University Research Reactor flux trap. These sources, which yield 1.2×10^{10} photons/s for the 46.5-keV (0.2667 Å) Mössbauer transition in ^{183}W, are approximately 1000 times more intense than conventional Mössbauer sources. This high intensity allows collimation to provide high angular resolution, giving momentum resolutions of 0.01, 0.1, and 1.0 Å^{-1} in the transverse, longitudinal, and vertical directions, respectively.[4] In the present experiments, 6-mm$\times$2.5-cm collimators were used before and after the sample which limited the angular divergences to 5 and 30 mrad in the horizontal and vertical directions, respectively. The energy analyses of the scattered photons were performed by Doppler shifting the Mössbauer absorber. The scattered beam passed (twice) through a natural W foil, 25 μm thick, which was mounted circumferentially on a rotor that was driven at velocities ranging from 0.65 to 262 cm/s, corresponding to energy shifts from 0.5 to 100 GHz. The 4.7-cm/s (1.8-GHz) width of the ^{183}W Mössbauer resonance for our experimental conditions defined the effective instrumental resolution. An intrinsic Ge detector provided near 100% detection efficiency and allowed energy separation of the 46.5-keV γ rays from others present in the spectrum.

Temperature control for the sample was provided by a heated bath and circulator with a 50-50 mixture of ethylene glycol and water for below ambient temperatures and water alone for those above it. The fluid was circulated through a copper coil soldered to the inner sample cell as shown in Fig. 2. Sample temperatures were determined by a Pt resistor attached to the inner sample cell. To minimize scattering from the cell windows, Kapton polymer films with a thickness of 50 μm were used. No Mössbauer signal was observed when the cell was filled with water. A pentadecane sample with a thickness of 4.4 cm was used which corresponded to a beam transmission of 50%.

Figure 3 shows the first maximum in the liquid struc-

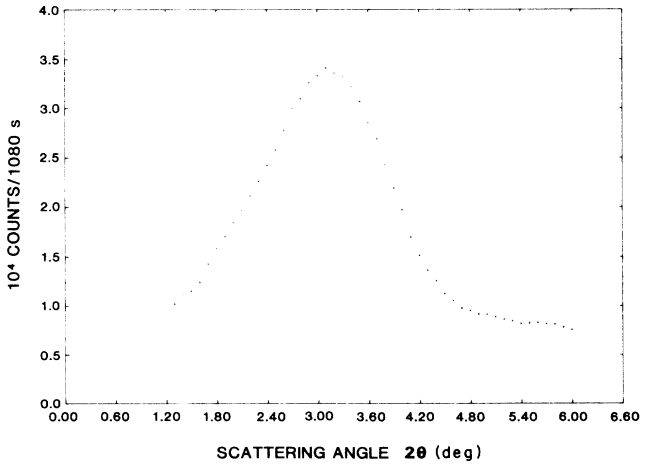

FIG. 3. The first maximum in the liquid structure factor at 12 °C.

TABLE I. Quasielastic linewidths Γ_2 measured for pentadecane at the temperatures and scattering vectors Q indicated. Relative amplitudes of the Lorentzian line shapes used to describe the elastic and quasielastic components of the Mössbauer signal are given by A_1/B and A_2/B, respectively. Numbers in parentheses are uncertainties.

Temperature °C	Counting time (h)	Q value (Å^{-1})	Two-Lorentzian fit[a] A_1/B (%)	A_2/B (%)	Γ_2 (GHz)
−10	24	1.15	22.7(0.20)		
12	233	1.15	0.13(0.07)	1.40	16.1(0.39)
15	82	1.15	0.20(0.10)	1.18	20.2(1.03)
24	108	1.15	0.19(0.10)	1.05	21.4(1.46)
38	120	1.15	0.01(0.11)	0.86	27.3(2.49)
74	242	1.15	0.06(0.05)	0.49	48.4(2.35)
12	80	0.82	0.57(0.15)	1.38	16.3(1.02)
12	215	1.00	0.25(0.07)	1.38	16.4(0.51)
12	233	1.15	0.13(0.07)	1.40	16.1(0.39)
12	221	1.41	0.23(0.07)	1.07	21.3(0.75)
12	79	1.56	0.00(0.01)	0.93	25.2(1.93)

[a]In all of the runs except at −10 °C, the width of the first Lorentzian was fixed equal to the instrumental resolution for elastic scattering measured for each source. The $A_2\Gamma_2/B$ product was constrained to an average value in the analyses.

ture factor or static structure factor $S(Q)$ at 12 °C. Mössbauer velocity spectra were recorded at different scattering angles and at different sample temperatures as reported in Table I. Figure 4 shows a typical velocity spectrum. In order to avoid source decay corrections, individual velocity scans with increasing velocities were added pairwise to scans with decreasing velocities. This method of data collection was an excellent approximation for the half-hour scan times used. As can be seen in Table I, total counting times per setting for the liquid measurements range between three and ten days.

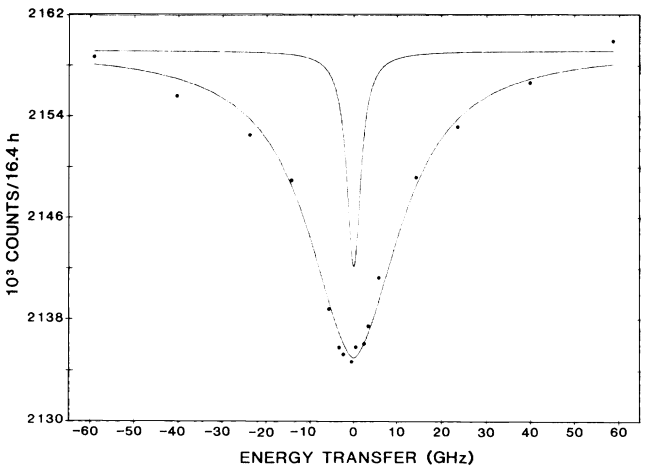

FIG. 4. Mössbauer velocity spectrum for scattering from pentadecane at 12 °C and $Q=1.15$ Å^{-1}. The narrow Lorentzian line shape shown represents the width for elastic scattering, but has been drawn with an arbitrary scale. The smooth curve through the data represents the two Lorentzian fit described in the text with the 0.13% elastic and 1.40% quasielastic components reported in Table I.

DATA ANALYSES

Quasielastically scattered Mössbauer photons were resonantly absorbed when the circumferential absorber on the rotor had the correct speed. These γ rays were therefore removed from the scattered beam and formed the QEGS signal which appeared as the minimum seen in Fig. 4. Primary analyses of the QEGS data consisted of fitting them with two Lorentzian line shapes plus continuum using a nonlinear least-squares fitting routine. The specific form used to parametrize $S(Q,\omega)$ was

$$\begin{aligned} I(Q,\omega) &= B - S(Q,\omega) \\ &= B - A_1(\Gamma_1/2)/[\omega^2+(\Gamma_1/2)^2] \\ &\quad - A_2(\Gamma_2/2)/[\omega^2+(\Gamma_2/2)^2] , \end{aligned} \tag{2}$$

where B was the constant continuum from which the Mössbauer signal was subtracted. The first Lorentzian corresponded to the small elastic scattering component due to frozen-in degrees of freedom in the sample, while the second corresponded to the quasielastic contribution. The width of the first Lorentzian Γ_1 was fixed equal to the instrumental resolution as determined each week for a freshly irradiated source by scattering from the 100% elastic, (200) Bragg reflection in LiF.[10] The width of the second Lorentzian Γ_2 was found from the fitting routine and was observed to reduce to Γ_1 when the sample temperature was lowered below the 10 °C freezing point. Amplitudes of the assumed Lorentzians relative to the continuum, A_1/B and A_2/B for the elastic and quasielastic components, respectively, are reported in Table I along with Γ_2. These ratios were used to get relative contributions rather than amplitude versus time, since the intensities of the sources used varied by factors of 2. As noted in the caption for Fig. 4, the scale chosen there for

the elastic component is arbitrarily large to better demonstrate its narrowness with respect to the quasielastic broadening. The widths reported actually include a small contribution from the instrumental resolution since no deconvolution scheme was used in Eq. (2). It is also worthwhile to note that in addition to absorber thickness, the true Mössbauer line shape depends on resonant self-absorption in the source[11] which is dependent upon its irradiation history. A source that has been irradiated several times, for example, will exhibit a broader resonance than a new source. This effect caused elastic widths to vary only between 1.7 and 1.95 GHz, as approximated by a simple Lorentzian. The magnitude of these non-Lorentzian effects for the present experiments was quite small with respect to the quasielastic broadening and made the above form used in Eq. (2) appropriate.

The data shown in Fig. 4 were taken at a scattering angle of 2.8° ($Q=1.15$ Å^{-1}), which was near the peak of the first maximum in the liquid structure factor shown in Fig. 3 for a temperature of 12 °C. The data points in Fig. 3, as well as the results reported in Table I, have been corrected for the non-46.5-keV radiation occurring within the single channel analyzer window used to select the γ-ray pulses. This correction was a nominal 25% effect except at small scattering angles near the unscattered beam. Measurements of $S(Q)$ at the other temperatures employed showed no appreciable differences from the 12 °C data. This lack of a temperature dependence for $S(Q)$ implied that the quasielastic intensity, as measured by the $A_2\Gamma_2/B$ product, should remain constant. When the data were analyzed in the manner described above by fitting on A_2 and Γ_2 independently, the $A_2\Gamma_2/B$ product varied by a factor of 1.6. It was noted, however, that if the product were constrained to an average value, the quality of the results from the least-squares fitting routine, as monitored by the weighted χ^2 value, was affected very little and in about half of the cases was actually improved (because of one less parameter). The values reported in Table I were then obtained by fitting on Γ_2 while constraining the $A_2\Gamma_2/B$ product to a weighted average value. The uncertainties quoted for A_1/B and Γ_2 in Table I were determined from the fitting routine.

In addition to the temperature dependence of the quasielastic broadening, a series of runs were taken at 12 °C to measure the Q dependence. Data were collected at scattering angles of 2.0°, 2.43°, 2.8°, 3.44°, and 3.8° corresponding to Q values of 0.82, 1.00, 1.15, 1.41, and 1.56 Å^{-1}, respectively, and were analyzed in the manner described above using two Lorentzians, but constraining the $A_2\Gamma_2/B$ product. The results of these runs are given in the lower part of Table I.

Since $S(Q)=\int S(Q,\omega)d\omega=\pi A_2\Gamma_2/2$ depends on Q, some additional comments about constraining the $A_2\Gamma_2/B$ product seem appropriate. The γ rays incident on the sample can be characterized as resonant (R) and nonresonant (NR) depending on whether they are emitted without recoil or with recoil, respectively. In addition to quasielastic and elastic scattering by the sample, which lead to the broad and narrow components of the Mössbauer signal shown in Fig. 4, there may also be inelastic (or phonon) processes, which would be extremely broad with respect to our velocity range (or completely outside of it). Since the cross section for inelastic processes is expected to be much less than that for quasielastic scattering for the Q and ω ranges used in this investigation, then $S(Q)$ measured for NR γ rays would be proportional to $S(Q,\omega)$ integrated over the quasielastic signal for the R γ rays. $S(Q)$ for NR γ rays is proportional to the continuum parameter B in Eq. (2). In fact, the data presented in Fig. 3 for $S(Q)$ were accumulated with the absorber velocity (ω) at an "off-resonance" or "continuum" value. Thus when the $A_2\Gamma_2/B$ ratio is formed, the Q dependence of the numerator is exactly compensated by the denominator to make this ratio independent of Q.

DISCUSSION

When the sample temperature was increased from the freezing point to 74 °C at constant Q, the quasielastic width Γ_2 was seen to increase from the elastic width near 2 GHz to 48 GHz as shown in Fig. 5. A monotonic behavior was expected, but remains to be quantitatively understood using computer simulations of molecular dynamics. Molecular-dynamics simulations on octane, for example,[12] give autocorrelation functions with relaxation times in the picosecond time range, but have not calculated the coherent structure factor.

From Eq. (1), however, simple theory predicts that Γ_2 would be directly proportional to $\sqrt{T}$. Since the sample showed only elastic scattering below its freezing point, indicating no quasielastic modes, the smooth curve shown on Fig. 5 was fitted to $\sqrt{T}$, where T was simply taken as the temperature above the freezing point. As can be seen on Fig. 5, the quasielastic widths seem to be better described by a linear relation with a finite value at the freez-

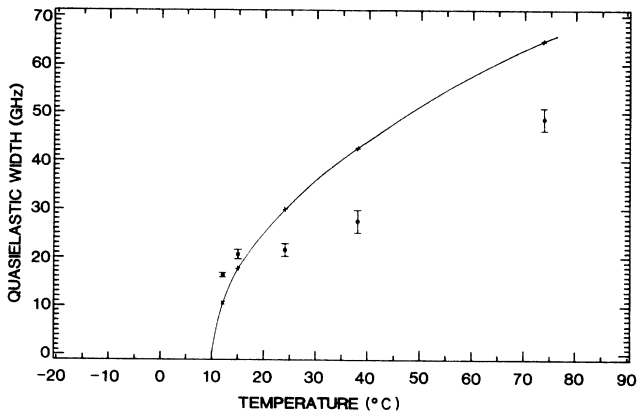

FIG. 5. Temperature dependence of the quasielastic width measured with QEGS at 1.15 Å^{-1}. These widths were extracted from the Mössbauer velocity spectra by fitting with two Lorentzians where the Γ_1 width was fixed equal to the instrumental width for elastic scattering, and the $A_2\Gamma_2/B$ products were constrained to the same average value.

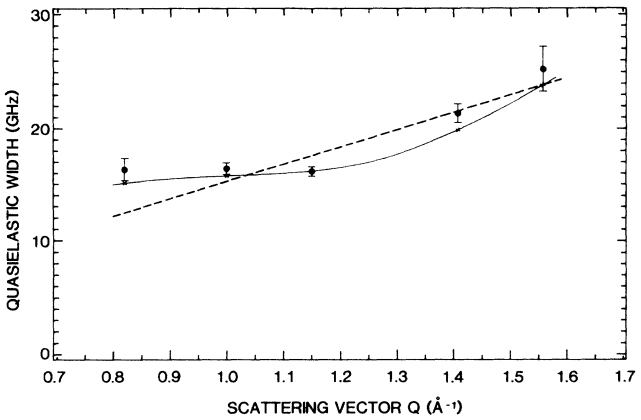

FIG. 6. Q dependence of the quasielastic width measured with QEGS at 12 °C. These widths were extracted from the Mössbauer velocity spectra by fitting with two Lorentzians where the Γ_1 width was fixed equal to the instrumental width for elastic scattering, and the $A_2\Gamma_2/B$ products were constrained to the same average value. The smooth curve is fit to $Q/\sqrt{S(Q)}$, which includes the de Gennes narrowing, whereas the dashed curve is simply fit to Q.

ing point than by the $\sqrt{T}$ dependence. In the QELS region, this dependence is known to be linear at low Q since the diffusion coefficient is directly proportional to T.

Although the QELS and QENS techniques give information that is not equivalent to QEGS, they are nevertheless similar enough to warrant comparisons and discussion. Depolarized Rayleigh light scattering has been extensively used to study quasielastic modes in hydrocarbons.[13,14] Contributions to the depolarized widths include molecular reorientation and diffusion (the narrowest width), and intermolecular collisions such as those that change chain conformations. Patterson reported[14] depolarized Rayleigh widths taken at $Q=0.00173$ Å^{-1} for a series of hydrocarbons; heptane, for instance, shows a width increase from 24 GHz at 30 °C to 45 GHz at 90 °C. No polarization analysis was performed in the present QEGS measurements.

Incoherent QENS measurements have also been reported on heptane.[15] A simple model[16] describing the dynamics as internal motions of the protons (jump, vibration, and rotation with respect to the center of mass) and diffusive motions of the whole molecule was used to interpret the incoherent QENS data. Proton jump lengths of 1.53 Å and internal relaxation times of order 3×10^{-12} s were extracted. It was also reported that "effective" diffusion coefficients (which contain contributions from intramolecular relaxations) were found to be a factor of 2 larger than the molecular self-diffusion coefficient as measured by other techniques. This leads to the conclusion that, even for low-viscosity liquids, internal modes contribute at least as much as molecular diffusion to quasielastic widths. For pentadecane, which has higher viscosity than pentane, the fraction of internal modes should be even higher. It should be noted that such a model[16] is not appropriate to understand our QEGS data because it does not describe coherent correlations measured by QEGS. However, until molecular-dynamics simulations are performed to interpret our data, it can be qualitatively stated that the main contributions to the widths reported here are due to local intermolecular and intramolecular nonpropagating modes (stretching, bending, twisting, and crankshaft motions) with some contribution from molecular self-diffusion. Brownian diffusion is believed to play a minor role for long-chain hydrocarbon liquids such as pentadecane, especially for temperatures not too high.

QELS has been characterized by two Brillouin lines (Stokes and anti-Stokes) due to hydrodynamic fluctuations in pressure at constant temperature.[2,7] These lines occur at frequencies $\omega=\pm QC_s$, where C_s is the adiabatic speed of sound. For QELS, such frequencies are observed at the wings of the Rayleigh line, whereas for QEGS or QENS they are at much higher frequency shifts (of order 5 THz at $Q=1$ Å^{-1}) and therefore outside of our instrument range. Moreover, such Brillouin lines are not expected to be observed above $Q=1$ Å^{-1} in simple liquids.[17]

When the A_1/B and A_2/B ratios for the elastic and quasielastic contributions to the Mössbauer signal reported in Table I are considered, two qualitative trends are apparent. First the A_1/B ratio is seen to decrease very sharply from 22.7% to less than 0.3% as the sample goes from a solid to a liquid. No significance is given to the fluctuations of this ratio above 12 °C. Second, the quasielastic A_2/B ratio is seen to decrease monotonically with increasing temperature as the width broadens. Recall that the $A_2\Gamma_2/B$ product has been constrained to an average value.

The quasielastic widths obtained for the Q-dependence data reported in Table I are graphed in Fig. 6. These widths follow a trend which is referred to as the de Gennes narrowing.[18] From the simple theory expressed by Eq. (1), the width in this case would be expected to be proportional to $Q/\sqrt{S(Q)}$. Using relative values for $S(Q)$ from Fig. 3, average values for $Q/\sqrt{S(Q)}$ have been used to draw the smooth curve on Fig. 6, which is seen to be in very good agreement with the experimental values. The rather broad experimental width for $S(Q)$ causes the smooth curve to "flatten out" around 1.1 Å^{-1} rather than give a "narrowing" or minimum in the width. If there were no de Gennes narrowing in this experiment, the data on Fig. 6 would be expected to follow the weighted, simple Q dependence shown by the dashed line.

The observed behavior of the width being inversely proportional to $\sqrt{S(Q)}$ has also been observed for coherent QENS data on atomic liquids [Ar (Ref. 19) and Rb (Ref. 17)] and for a mixed ionic glass.[20] A theoretical basis for such behavior has been presented for light interstitials in metals[21] and for macromolecules in dilute solutions.[22]

CONCLUSIONS

The newly developed QEGS technique opens possibilities for the study of quasielastic normal modes (sometimes called quasiphonons) in liquids and liquid mixtures.

Since QELS looks at micron scale lengths, the QEGS technique can complement it by yielding information at characteristic sizes of the order of interatomic distances and can also be used on nontransparent samples. QEGS can also complement QENS by giving purely coherent scattering data, since QENS measures a mixture of coherent and incoherent signals or mostly incoherent signals except for a few atomic liquids. The QEGS technique could be useful for studies of the effect of side groups and branching on the dynamics of liquid hydrocarbons, the monitoring of the freezing-in of the various degrees of freedom in marcomolecular melts and the dynamics characterization of the ordering transition in liquid crystals by separating elastic-quasielastic contributions.

ACKNOWLEDGMENTS

Useful discussions with Professor S. Aragon, Professor R. Pecora, and Professor K. Schmitz and help from Dr. W. B. Yelon and Mr. S. H. Kim are greatly appreciated. This material was prepared with the support of the U. S. Department of Energy, Grant No. DE-FG02-85ER-45200.

---

*Present address: U.S. Department of Commerce, Materials Science and Engineering Laboratory Building 235, E121, National Institute of Standards and Technology, Gaithersburg, MD 20899.

†Present address: Wyse Technology, San Jose, CA 95134.

[1]B. Berne and R. Pecora, *Dynamic Light Scattering with Applications to Chemistry, Biology and Physics* (Wiley-Interscience, New York, 1976).

[2]*Methods of Experimental Physics,* edited by R. Celotta and J. Levine (Academic, New York, 1988), Vol. 23.

[3]W. B. Yelon, G. Schupp, M. L. Crow, C. Holmes, and J. G. Mullen, Nucl. Instrum. Methods B **14**, 341 (1986).

[4]M. L. Crow, G. Schupp, W. B. Yelon, J. G. Mullen, and A. Djedid, Acta Crystallogr. A **43**, 638 (1987).

[5]M. L. Crow, G. Schupp, W. B. Yelon, J. G. Mullen, and A. Djedid, Phys. Rev. B **39**, 909 (1989).

[6]J. P. Hansen and I. R. McDonald, *Theory of Simple Liquids* (Academic, New York, 1976).

[7]J. S. Boon and S. Yip, *Molecular Hydrodynamics* (McGraw-Hill, New York, 1980).

[8]D. St. P. Bunbury, J. A. Elliott, H. E. Hall, and J. M. Williams, Phys. Lett. **6**, 34 (1963).

[9]P. P. Craig and N. Suttin, Phys. Rev. Lett. **11**, 460 (1963).

[10]J. G. Mullen and J. R. Stevenson, *Workshop on New Directions in Mössbauer Spectroscopy, Argonne, 1977* in Proceedings of the Workshop on New Directions in Mössbauer Spectroscopy, AIP Conf. Proc. No. **38**, edited by G. J. Perlow (AIP, New York, 1977), p. 55.

[11]J. G. Mullen, A. Djedid, G. Schupp, D. Cowan, Y. Cao, M. L. Crow, and W. B. Yelon, Phys. Rev. B **37**, 3226 (1988).

[12]T. W. Weber, J. Chem. Phys. **70**, 4277 (1979).

[13]G. D. Patterson, C. P. Lindsey, and G. R. Alms, J. Chem. Phys. **69**, 3250 (1978).

[14]G. D. Patterson and P. J. Carroll, J. Chem. Phys. **76**, 4356 (1982).

[15]K. E. Larsson, L. Q. do Amaral, N. Ivanchev, S. Ripeanu, L. Bergstedt, and U. Dahhlborg, Phys. Rev. **151**, 126 (1966).

[16]K. E. Larsson and L. Bergstedt, Phys. Rev. **151**, 117 (1966).

[17]J. R. D. Copley and S. W. Lovesey, Rep. Prog. Phys. **38**, 461 (1975).

[18]P. G. de Gennes, Physica **25**, 825 (1959).

[19]K. Skold, J. M. Rowe, G. Ostrowski, and P. D. Randolph, Phys. Rev. A **6**, 1107 (1972).

[20]F. Mezei, W. Knaak, and B. Farago, Phys. Scr. **T19**, 363 (1987).

[21]S. K. Sinha and D. K. Ross, Physica B **149**, 51 (1988).

[22]A. Z. Akcasu and H. Gurol, J. Polym. Sci. Polym Phys. Ed. **14**, 1 (1976).